Stress-energy tensor of quantized scalar fields in a zero-tidal wormhole

Shun Jiang [*] and Jie Jiang [†]

School of Physics and Optoelectronics, South China University of Technology, Guangzhou 510641, China and Faculty of Arts and Sciences, Beijing Normal University, Zhuhai 519087, China

(Received 24 February 2026; accepted 4 June 2026; published 6 July 2026)

To create a static traversable wormhole, exotic matter that meets the Morris-Thorne conditions is required. It is well known that the expectation value of the vacuum stress-energy tensor can violate the null energy condition and thus has long been considered the best candidate for exotic matter. In this paper, we investigate whether the renormalized stress-energy tensor of a nonminimally coupled massive scalar field in a zero-tidal wormhole can satisfy the Morris-Thorne conditions. Within the Hadamard renormalization framework, we calculate the renormalized stress-energy tensor using the pragmatic mode-sum regularization method recently established by Levi and Ori. By varying the dimensionless scalar field mass and coupling constant, we find that there are three disconnected regions in this two-dimensional parameter space that satisfy the Morris-Thorne conditions. We identify two intervals in the dimensionless scalar field mass, within which the Morris-Thorne conditions cannot be satisfied irrespective of the value of the coupling constant. This establishes two mass exclusion regions that constitute a no-go regime for the construction of traversable wormholes.

DOI: 10.1103/h7d6-9yq4

I. INTRODUCTION

The concept of traversable wormholes was brought into the physical domain by Morris and Thorne [1] in 1988. To maintain the structure of a wormhole, they found that the matter at the wormhole throat needs to satisfy the Morris-Thorne conditions, and this will lead to a violation of energy conditions. Because of this exotic behavior, they referred to the matter at the wormhole throat as exotic matter. It is well known that the quantum stress-energy tensor can violate energy conditions. Accordingly, Morris *et al.* first supposed that it could serve as a candidate for exotic matter [2].

To investigate whether a quantum scalar field can serve as exotic matter, analytical approximations of the quantum stress-energy tensor has been employed to examine whether the Morris-Thorne conditions can be satisfied [3–10]. Using analytic approximation expression of the quantum stress-energy tensor [11], the first wormhole solution of the semiclassical Einstein field equations has been obtained in [12]. The expectation value of ϕ^2 for the thermal state is calculated in the short-throat wormhole [13]. By introducing additional boundaries, the Casimir effect is employed to investigate whether it can serve as the exotic matter required for wormholes [14,15]. Calculating the exact quantum vacuum energy-momentum tensor has always been a difficult task. To avoid this difficulty, a short-throat flat-space wormhole model has been studied in [16]. This model consists of two identical copies of Minkowski space, each with spherical regions excised, whose boundaries are to be identified. Thus, the spacetime is everywhere flat except a two-dimensional singular spherical surface. Within this model setup, the vacuum stress-energy tensor has been obtained [16]. It represents an infinitesimally thin exotic matter layer at the wormhole throat, indicating a discontinuous distribution in spacetime. To gain a deeper understanding of the behavior of the quantum stress-energy tensor at the wormhole throat, it is natural to calculate the exact renormalized vacuum stress-energy tensor in more realistic wormhole models.

The naive computation of the quantum stress-energy tensor leads to a divergent result. Thus, renormalization must be considered, which constitutes the primary challenge in computing the quantum stress-energy tensor. Using the point-splitting method [17,18], the expression for the divergent terms of the energy-momentum tensor was obtained in [19]. In 1984, Candelas and Howard [20] developed a method to calculate the expectation value of ϕ^2. They applied this method to compute the expectation value of ϕ^2 in Schwarzschild spacetime [20]. Subsequently, Howard [21] used this method to calculate the expectation value of the stress-energy tensor in Schwarzschild spacetime. This approach involves using a Wick rotation to convert the Lorentzian metric into a Euclidean one. Recently, Levi and Ori [22,23] proposed the pragmatic mode-sum regularization method for computing the renormalized stress-energy tensor. This approach allows direct calculations in Lorentzian backgrounds. When applying the point-splitting technique in the two aforementioned regularization methods, it is

[*]Contact author: shunjiang@mail.bnu.edu.cn
[†]Contact author: jiejiang@mail.bnu.edu.cn

necessary to subtract the corresponding counterterms to remove the divergences. In [19], the explicit expression of the counterterm is provided. However, it takes the form of a power series in terms of $1/m_0^2$, which is inconvenient for explicit calculations. The Hadamard renormalization approach directly computes the divergent terms by exploiting the singular structure of the two-point correlation function, thereby avoiding the computational complexity arising from series expansions. The Hadamard renormalization for a quantized scalar field has been developed in [24]. By employing the bitensor expansion technique outlined in [19] and the geometric expressions given in Ref. [24], one can in principle derive the counterterms required for Hadamard renormalization.

To our best knowledge, the exact vacuum quantum stress-energy tensor for wormholes has so far been calculated only under the short-throat flat-space approximation [16]. To investigate whether it can sustain the wormhole throat, we must transition to more realistic wormhole models. In this paper, we study the renormalized stress-energy tensor of a massive scalar field with nonminimal coupling at the throat of a zero-tidal wormhole, which is the simplest traversable wormhole with zero radial tides. Within the Hadamard renormalization framework [24], we employ the mode-sum regularization method developed by Levi and Ori [22,23] to compute the renormalized stress-energy tensor. We explore the parameter space of the dimensionless scalar field's mass and coupling constant to identify regions where the Morris-Thorne conditions are fulfilled.

This paper is organized as follows. In Sec. II, we briefly review the Morris-Thorne conditions and the zero-tidal wormholes. In Sec. III, we quantize scalar fields in a zero-tidal wormhole spacetime. In Sec. IV, we numerically calculate the renormalized stress-energy tensor and examine whether it satisfies the Morris-Thorne conditions at the wormhole throat. In Sec. V, we discuss the results.

II. ZERO-TIDAL WORMHOLES AND THE MORRIS-THORNE CONDITIONS

In this section, we first briefly review the general traversable wormhole model, as well as the energy conditions required for traversable wormholes, namely the Morris-Thorne conditions. Then, we introduce the zero-tidal wormhole model, the simplest traversable wormhole with zero radial tides we will consider in this paper.

The metric of the static and spherically symmetric wormhole can be written as [1]

$$ds^2 = -e^{2\Phi(r)}dt^2 + \left(1 - \frac{b(r)}{r}\right)^{-1} dr^2 + r^2 d\Omega^2. \quad (1)$$

Here $\Phi(r)$ is the redshift function and $b(r)$ is the shape function. To achieve the traversable wormhole geometry, $\Phi(r)$ and $b(r)$ are required to satisfy the following conditions [1]:

(A1) There exists an $r_0 > 0$ such that $b(r_0) = r_0$ and $1 - \frac{b(r)}{r} \geq 0$ for $r \geq r_0$.

(A2) $\frac{d^2 r}{dr_*^2} > 0$ near r_0, where $r_*(r) = \pm \int_{r_0}^{r} (1 - \frac{b(r)}{r})^{-\frac{1}{2}} dr$ is the proper radial distance.

(A3) $\Phi(r)$ is everywhere finite.

Items (A1) and (A2) imply the existence of a wormhole throat at $r = r_0$. Item (A3) ensures the absence of a horizon, thereby rendering the wormhole traversable.

Now, let us consider what kind of stress-energy tensor is required for traversable wormholes. Let $\{e_u^a\}$ be an orthonormal tetrad corresponding to the static observer, which can be written as

$$e_0^a = e^{-\Phi(r)} \left(\frac{\partial}{\partial t}\right)^a, \qquad e_1^a = \left(1 - \frac{b(r)}{r}\right)^{\frac{1}{2}} \left(\frac{\partial}{\partial r}\right)^a,$$
$$e_2^a = \frac{1}{r}\left(\frac{\partial}{\partial \theta}\right)^a, \qquad e_3^a = \frac{1}{r\sin\theta}\left(\frac{\partial}{\partial \phi}\right)^a. \quad (2)$$

Using this set of frames, the Einstein field equations can be written as

$$\rho = T_{00} = \frac{1}{8\pi r^2}\frac{d}{dr}b(r), \quad (3)$$

$$\tau = -T_{11} = \frac{1}{8\pi}\left[\frac{b}{r^3} - \frac{2}{r}\left(1 - \frac{b}{r}\right)\frac{d}{dr}\Phi(r)\right], \quad (4)$$

$$p = T_{22} = T_{33} = \frac{r}{2}\left[(\rho - \tau)\frac{d}{dr}\Phi(r) - \frac{d}{dr}\tau\right] - \tau. \quad (5)$$

Using items (A1)–(A3), the conditions for making a wormhole traversable can be expressed as

$$\tau_0 > 0, \quad (6)$$

$$\eta_0 = \tau_0 - \rho_0 > 0, \quad (7)$$

where $\tau_0 = \tau|_{r=r_0}$ and $\rho_0 = \rho|_{r=r_0}$. Conditions (6) and (7) are called the Morris-Thorne conditions. The difficulty is that the Morris-Thorne conditions are not easily satisfied. From condition (6), we can see that $\tau > 0$ implies a tension exists at the wormhole throat, rather than a pressure as would correspond to a perfect fluid for $\tau < 0$. Furthermore, condition (7) leads to the violation of energy conditions by the matter at the wormhole throat. Therefore, matter satisfying conditions (6) and (7) is referred to as exotic matter. It is well known that the vacuum energy-momentum tensor in quantum field theory can violate energy conditions. Thus, quantum vacuum fluctuations might maintain the geometric structure of a wormhole.

In this paper, we consider the zero-tidal wormhole which is the simplest traversable wormhole with the zero radial tides. By choosing $\Phi(r) = 0$ and $b(r) = b_0$ in (1), the line element of the zero-tidal wormhole can be written as

$$ds^2 = -dt^2 + \left(1 - \frac{b_0}{r}\right)^{-1} dr^2 + r^2 d\Omega^2. \tag{8}$$

To explore the parameter space of spacetime and scalar fields, we will consider the Morris-Thorne conditions within the dimensionless $m_0 b_0 - \xi$ parameter space.

III. QUANTUM FIELD THEORY IN WORMHOLE SPACETIME

In this section, we shall quantize scalar fields in the zero-tidal wormhole spacetime and derive the expression of the renormalized energy-momentum tensor. Detailed calculation procedures are provided in Appendix A.

We begin by reviewing the classical Klein-Gordon scalar field. The associated action is given by

$$S = -\frac{1}{2}\int d^4x\sqrt{-g}(g^{ab}\nabla_a\phi\nabla_b\phi + m_0^2\phi^2 + \xi R\phi^2), \tag{9}$$

where m_0 is the mass of the scalar field and ξ is the coupling constant of the scalar field. The equation for a nonminimally coupled massive scalar field can be written as

$$(\nabla_a\nabla^a - m_0^2 - \xi R)\phi = 0. \tag{10}$$

The stress-energy tensor is given by

$$\begin{aligned} T_{uv} = {} & (1-2\xi)\phi_{;u}\phi_{;v} + \left(2\xi - \frac{1}{2}\right) g_{uv} g^{\rho\sigma}\phi_{;\rho}\phi_{;\sigma} - 2\xi\phi\phi_{;uv} \\ & + 2\xi g_{uv}\phi\nabla_a\nabla^a\phi + \xi\left(R_{uv} - \frac{1}{2}R g_{uv}\right)\phi^2 \\ & - \frac{1}{2} g_{uv} m_0^2\phi^2. \end{aligned} \tag{11}$$

Now, we quantize the Klein-Gordon scalar field. Using spherical symmetry, the mode functions can be written as

$$\psi_{\omega lm}(t,r,\theta,\varphi) = \frac{1}{\sqrt{4\pi|\omega|}} e^{-i\omega t} Y_{lm}(\theta,\varphi)\frac{R_{\omega l}(r)}{r}. \tag{12}$$

The radial function $R_{\omega l}(r)$ satisfies the following equation:

$$\frac{d^2 R_{\omega l}}{dr_*^2} + (\omega^2 - V_{\rm eff})R_{\omega l} = 0, \tag{13}$$

where the r_* is the proper radial distance which is defined in (A2) of Sec. II and the effective potential is given by

$$\begin{aligned} V_{\rm eff}(r) = f(r)\Bigg(& m_0^2 + \xi R + \frac{l(l+1)}{r^2} \\ & + \frac{1}{r\sqrt{f(r)h(r)}}\frac{d}{dr}\left(\sqrt{\frac{f(r)}{h(r)}}\right)\Bigg). \end{aligned} \tag{14}$$

Here we take

$$f(r) = 1, \qquad h(r) = \left(1 - \frac{b_0}{r}\right)^{-1}. \tag{15}$$

Following [25], we choose two linearly independent basis functions for Eq. (13), denoted $R^L_{\omega l}$ and $R^R_{\omega l}$. $R^L_{\omega l}$ and $R^R_{\omega l}$ correspond to the waves coming from $r_* \to -\infty$ and $r_* \to \infty$, respectively. The boundary conditions for $R^L_{\omega l}$ and $R^R_{\omega l}$ are given by

$$\begin{aligned} R^L_{\omega l} &= \begin{cases} e^{i\sqrt{\omega^2 - m_0^2} r_*} + \mathcal{R}^L_{\omega l} e^{-i\sqrt{\omega^2 - m_0^2} r_*}, & r_* \to -\infty, \\ \mathcal{T}^L_{\omega l} e^{i\sqrt{\omega^2 - m_0^2} r_*}, & r_* \to \infty, \end{cases} \\ R^R_{\omega l} &= \begin{cases} e^{-i\sqrt{\omega^2 - m_0^2} r_*} + \mathcal{R}^R_{\omega l} e^{i\sqrt{\omega^2 - m_0^2} r_*}, & r_* \to \infty, \\ \mathcal{T}^R_{\omega l} e^{-i\sqrt{\omega^2 - m_0^2} r_*}, & r_* \to -\infty. \end{cases} \end{aligned} \tag{16}$$

Thus, we have two linearly independent mode functions $\psi^L_{\omega lm}$ and $\psi^R_{\omega lm}$ which are given by

$$\psi^{L/R}_{\omega lm}(t,r,\theta,\varphi) = \frac{1}{\sqrt{4\pi|\omega|}} e^{-i\omega t} Y_{lm}(\theta,\varphi)\frac{R^{L/R}_{\omega l}(r)}{r}. \tag{17}$$

The field operator can then be conveniently expressed as

$$\begin{aligned} \hat{\phi}(x) = \int_0^\infty dk \sum_{l=0}^{\infty}\sum_{m=-l}^{m=l} \Big(& a^L_{\omega(k)lm}\psi^L_{\omega(k)lm}(x) \\ & + a^R_{\omega(k)lm}\psi^R_{\omega(k)lm}(x) + a^{L\dagger}_{\omega(k)lm}\psi^{L*}_{\omega(k)lm}(x) \\ & + a^{R\dagger}_{\omega(k)lm}\psi^{R*}_{\omega(k)lm}(x)\Big). \end{aligned} \tag{18}$$

Here $\omega(k) = \sqrt{m_0^2 + k^2}$.

The vacuum state $|0\rangle$, corresponding to the annihilation operators $a^L_{\omega(k)lm}$ and $a^R_{\omega(k)lm}$, is defined by

$$a^L_{\omega(k)lm}|0\rangle = 0, \qquad a^R_{\omega(k)lm}|0\rangle = 0. \tag{19}$$

In Appendix A, we derive the expression for the renormalized energy-momentum tensor $T_{uv,\rm rem}$ using Hadamard renormalization, which can be expressed as

$$
\begin{aligned}
T_{uv,\mathrm{rem}}(x) = \frac{v_1}{4\pi^2} g_{uv} + \lim_{x'\to x}\bigg[&(1-2\xi)\left(g_v{}^{v'} G(x,x')_{;uv'} - g_v{}^{v'} C(x,x')_{;uv'}\right) \\
&+\left(2\xi-\frac{1}{2}\right) g_{uv}\left(g^{\rho\sigma'} G(x,x')_{;\rho\sigma'} - g^{\rho\sigma'} C(x,x')_{;\rho\sigma'}\right) - 2\xi\left(g_u{}^{u'} g_v{}^{v'} G(x,x')_{;u'v'} - g_u{}^{u'} g_v{}^{v'} C(x,x')_{;u'v'}\right) \\
&+2\xi g_{uv}(G(x,x')_{;\rho}{}^{;\rho} - C(x,x')_{;\rho}{}^{;\rho}) + \xi\left(R_{uv} - \frac{1}{2} R g_{uv}\right)(G(x,x') - C(x,x')) - \frac{1}{2} m_0^2 g_{uv}(G(x,x') - C(x,x'))\bigg].
\end{aligned}
\tag{20}
$$

IV. THE RENORMALIZED STRESS-ENERGY TENSOR AND MORRIS-THORNE CONDITIONS

In this section, we utilize the pragmatic mode-sum regularization method [22,23] within the Hadamard renormalization framework [24] to calculate the renormalized stress-energy tensor for a scalar field at the throat of the zero-tidal wormhole. We vary the dimensionless scalar field mass $m_0 b_0$ and coupling coefficient ξ of the scalar field to analyze whether the quantum vacuum stress-energy tensor satisfies the Morris-Thorne conditions.

A. Setup

The expression for the renormalized stress-energy tensor is given by (20). For computational convenience, we need to rewrite (20) in a more manageable form. The detailed calculations are provided in Appendix B. Then the renormalized stress-energy tensor (20) can be written as

$$
\begin{aligned}
T_{uv,\mathrm{rem}}(x) = (1-2\xi) G_{1uv,\mathrm{rem}}(x) + \left(2\xi - \frac{1}{2}\right) g_{uv} g^{\rho\tau} G_{1\rho\tau,\mathrm{rem}}(x) - 2\xi G_{2uv,\mathrm{rem}}(x) \\
+ 2\xi g_{uv} g^{\rho\tau} G_{0uv,\mathrm{rem}} + \xi\left(R_{uv} - \frac{1}{2} R g_{uv}\right) G_{\mathrm{rem}} - \frac{1}{2} m_0^2 g_{uv} G_{\mathrm{rem}} + \frac{v_1}{4\pi^2} g_{uv}.
\end{aligned}
\tag{21}
$$

The definitions of notations $G_{iuv,\mathrm{rem}}$ and G_{rem} are provided in Appendix B and the explicit expressions are given in (B18)–(B20) and (B23). These expressions provide us with a convenient form for calculating the stress-energy tensor.

Now, we turn to the calculation of the renormalized stress-energy tensor (21) using the pragmatic mode-sum regularization method [22,23]. We need to compute the values of $G_{iuv,\mathrm{rem}}$ and G_{rem} defined in (B18)–(B20) and (B23). Since the calculation processes for these terms are very similar, we will present the detailed procedure for $G_{1uv,\mathrm{rem}}$ as an example.

The explicit form of $G_{1uv,\mathrm{rem}}$ is derived in Appendix B, which can be expressed as

$$
\begin{aligned}
G_{1uv,\mathrm{rem}}(x) = \int_0^\infty \left[F_{1uv}(x,k) - \frac{k}{\sqrt{k^2+m_0^2}} F_{1uv,\mathrm{sing}}(x,\omega(k))\right] dk \\
- \int_0^{m_0} F_{1uv,\mathrm{sing}}(x,\omega(k)) d\omega - e_{1uv}(x).
\end{aligned}
\tag{22}
$$

Using (17) and (B12), the specific forms of the components of F_{1uv} can be written as

$$
\begin{aligned}
F_{1\mathrm{tt}}(x,k) &= \sum_{l=0}^{\infty} \sum_{m=-l}^{m=l} \frac{\omega}{4\pi r^2} |Y_{lm}(\theta,\varphi)|^2 (|R_{\omega l}^L|^2 + |R_{\omega l}^R|^2) \\
F_{1r_*r_*} &= \sum_{l=0}^{\infty} \sum_{m=-l}^{m=l} \frac{1}{4\pi\omega} |Y_{lm}(\theta,\varphi)|^2 \left(\left|\frac{d}{dr_*}\left(\frac{R_{\omega l}^L}{r}\right)\right|^2 + \left|\frac{d}{dr_*}\left(\frac{R_{\omega l}^L}{r}\right)\right|^2\right) \\
F_{1\varphi\varphi}(x,k) &= \sum_{l=0}^{\infty} \sum_{m=-l}^{m=l} \frac{1}{4\pi\omega r^2} |Y_{lm,\varphi}(\theta,\varphi)|^2 (|R_{\omega l}^L|^2 + |R_{\omega l}^R|^2),
\end{aligned}
\tag{23}
$$

where $R^L_{\omega(k)lm}(x)$ and $R^R_{\omega(k)lm}(x)$ satisfy the radial equation (13), with their boundary conditions given by (16). The value of $F_{1\theta\theta}$ can be derived from $F_{1\varphi\varphi}$ by exploiting spherical symmetry. The summation over m in (23) can be evaluated using the following identities:

$$\sum_{m=-l}^{m=l} |Y_{lm}(\theta,\varphi)|^2 = \frac{2l+1}{4\pi},$$
$$\sum_{m=-l}^{m=l} |Y_{lm,\varphi}(\theta,\varphi)|^2 = \frac{l(l+3l+2l^2)}{8\pi}. \tag{24}$$

The explicit form of $F_{1uv,\mathrm{sing}}$ is given in Appendix B and can be expressed as

$$F_{1uv,\mathrm{sing}}(x,\omega) = \frac{1}{6}a_{1uv}(x)\omega^3 - b_{1uv}(x)\omega - \frac{2}{\pi}c_{1uv}(x)\log(\omega) - d_{1uv}(x)\frac{1}{\omega+e^{-\gamma}}. \tag{25}$$

Here the explicit forms of a_{1uv}, b_{1uv}, c_{1uv}, d_{1uv}, and e_{1uv} [from (22)] are given in (B26).

B. Numerical results

In this subsection, we numerically compute the renormalized energy-momentum tensor $T_{uv,\mathrm{rem}}$ given by (21). To achieve this goal, we need to compute the values of $G_{iuv,\mathrm{rem}}$ and G_{rem} as given in (21). As discussed in the previous subsection, the computations of $G_{iuv,\mathrm{rem}}$ and G_{rem} are highly similar; for concreteness, we focus on $G_{1uv,\mathrm{rem}}$, whose explicit form was already derived in the preceding subsection.

To calculate $G_{1uv,\mathrm{rem}}$ given by (22), we need to numerically compute F_{1uv}. The expression for F_{1uv} is given by (23). Accordingly, we need to numerically compute the mode functions $R^L_{\omega(k)lm}$ and $R^R_{\omega(k)lm}$, which satisfy (13) and are subject to the boundary conditions specified in (16).

By numerically solving the radial equation (13) with the given boundary conditions (16), we obtain $R^L_{\omega(k)lm}(x)$ and $R^R_{\omega(k)lm}(x)$ for k between 0 and 60 with a uniform step of $dk = 1/20$. For any fixed ω, we sum over l in (23) until the corresponding contribution falls below 10^{-12}.

Figure 1 presents the numerical results of $F_{1\mathrm{tt}}$ for $r = r_0$ with $m_0 = 0$. As can be seen from Fig. 1, $F_{1\mathrm{tt}}$ increases with the growth of k, thus directly integrating it will lead to divergence. The divergence arises from the two-point correlation function satisfying the Hadamard condition (A2). For computational convenience, we consider the symmetric two-point function $\omega_{2,\mathrm{sym}}$ given by (A3). After this symmetrization operation, the expressions of the first two terms in Eq. (A2) become those in Eq. (A5). When calculating the expectation value of $\hat{\phi}^2$, we set $x \to x'$, which causes $\sigma \to 0$ and thus leads to the divergence of the first two terms in (A5).

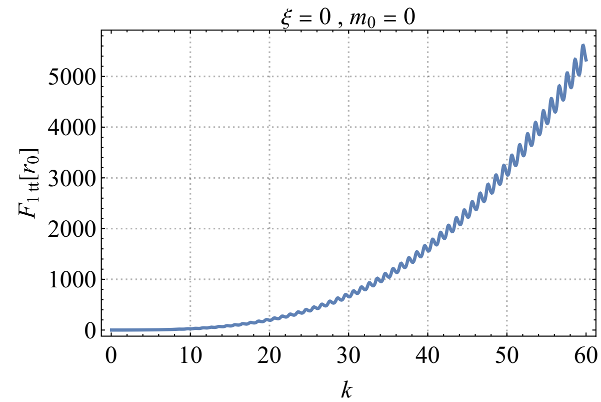

FIG. 1. The curve in this figure displays the value of $F_{1\mathrm{tt}}$ for $r = r_0$, $\xi = 0$, and $m_0 = 0$ in the zero-tidal wormhole.

This kind of divergence naturally enters the calculation of the expectation value of the energy-momentum tensor, since the energy-momentum tensor is obtained by taking derivatives of the two-point correlation function. The $F_{1\mathrm{tt}}$ in Fig. 1 grows rapidly as k increases, which numerically confirms the existence of this divergence. Therefore, renormalization is required. Since the expression for the energy-momentum tensor (A11) involves an integral over the mode functions, we need to also express the divergent term (A5) and its corresponding form in the energy-momentum tensor expression as an integral. We provide the detailed calculation in Appendix B.

By subtracting the divergent part $F_{1\mathrm{tt,sing}}(x,\omega(k))$ given by (B17), we define two quantities

$$F_{1\mathrm{ttreg}}(x,k) = F_{1\mathrm{tt}}(x,k) - \frac{k}{\sqrt{k^2+m_0^2}}F_{1\mathrm{tt,sing}}(x,\omega(k)) \tag{26}$$

and

$$H_{1\mathrm{tt}}(x,k) = \int_0^k \left[F_{1\mathrm{tt}}(x,k_1) - \frac{k_1}{\sqrt{k_1^2+m_0^2}}F_{1\mathrm{tt,sing}} \times (x,\omega(k_1))\right]dk_1. \tag{27}$$

Figure 2 presents the numerical results of $F_{1\mathrm{ttreg}}$ for $r = r_0$ with $m_0 = 0$. A comparison between Figs. 1 and 2 shows that the divergence of $F_{1\mathrm{ttreg}}$ relative to $F_{1\mathrm{tt}}$ has been substantially alleviated; this indicates that we have successfully eliminated the divergent component in $F_{1\mathrm{tt}}$ caused by $F_{1\mathrm{tt,sing}}$. Now, $F_{1\mathrm{ttreg}}$ exhibits strong oscillatory characteristics. To verify whether $F_{1\mathrm{ttreg}}$ converges after integration, we perform an integration on $F_{1\mathrm{ttreg}}$. Figure 3 displays the numerical results of $H_{1\mathrm{tt}}$ for $r = r_0$ with $m_0 = 0$ which is the integral value of the function $F_{1\mathrm{ttreg}}$ with respect to k. Comparing Figs. 2 and 3, we observe that the divergence is further weakened. However, the highly oscillatory nature

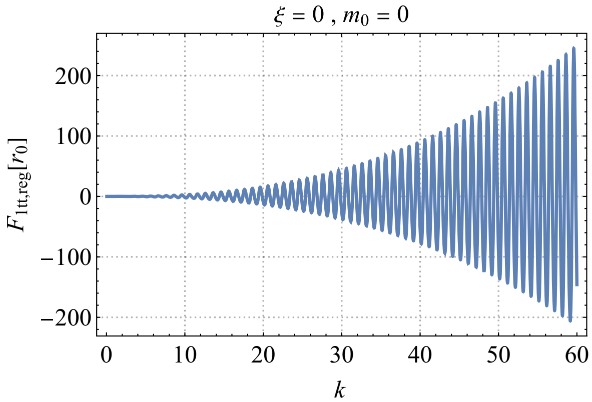

FIG. 2. The curve in this figure displays the value of $F_{1\mathrm{ttreg}}$ for $r = r_0$, $\xi = 0$, and $m_0 = 0$ in the zero-tidal wormhole.

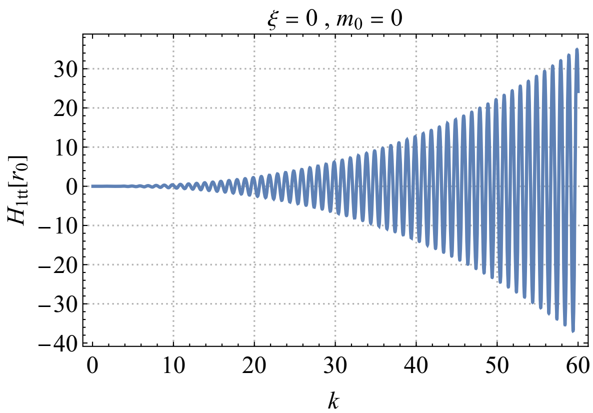

FIG. 3. The curve in this figure displays the value of $H_{1\mathrm{tt}}$ for $r = r_0$, $\xi = 0$, and $m_0 = 0$ in the zero-tidal wormhole.

does not vanish after the integration and the result still does not converge. The origin and nature of oscillations are presented in [22]. In essence, this phenomenon arises from the fact that a null geodesic emanating from a spatial point can return to that spatial point. Thus, we can find two spacetime points, $x = (t, r, \theta, \varphi)$ and $x' = (t + \epsilon, r, \theta, \varphi)$, that can be connected by a null geodesic. In such cases, σ in (A5) equals zero, which gives rise to a singularity. As shown in [22], when we convert these singularities into integral form, they exhibit the oscillatory behaviors. In fact, due to these divergent behaviors, we are actually dealing with an generalized integral. To handle such integrals, we need to employ the self-cancellation method developed in [22,23].

First, let us briefly review the self-cancellation method presented in [22,23]. To address such oscillatory integrals, at the analytical level, we can adopt the Abel-summed integral, where the value of the generalized integral of h is defined as the limit of the following expression:

$$\lim_{\epsilon\to 0^+} \int_0^\infty e^{-\epsilon\omega} h(\omega) d\omega, \tag{28}$$

where we assume that this integral exists for all $\epsilon > 0$ and that the limit exists as $\epsilon \to 0^+$. However, this is not suitable for numerical calculation, since in practice we can only evaluate $h(\omega)$ over a finite range $0 < \omega < \omega_{\max}$. To numerically handle the generalized integral, we need to employ the self-cancellation method. To introduce this method, we first define the integral

$$H(\omega) \coloneqq \int_0^\omega h(x) dx. \tag{29}$$

This method requires that the oscillations of $H(\omega)$ have well-defined frequencies. The H_{1tt} in Fig. 3 indeed satisfies this condition. If we assume the period of oscillation is λ, the self-cancellation operation T_λ is defined by

$$T_\lambda[H(\omega)] \coloneqq \frac{H(\omega) + H(\omega + \frac{\lambda}{2})}{2}. \tag{30}$$

To eliminate oscillations at a fixed frequency, we apply the cancellation procedure iteratively. Once oscillations at one dominant frequency are removed, the next oscillatory component—with relatively smaller amplitude—becomes dominant. We therefore sequentially eliminate the leading oscillatory modes until the remaining oscillations become negligible. This multiple self-cancellation operator can be written as

$$T_* \coloneqq (T_{\lambda_1})^{n_1} (T_{\lambda_2})^{n_2} \ldots (T_{\lambda_m})^{n_m}. \tag{31}$$

Therefore, in the self-cancellation method, the value of the generalized integral of $h(x)$ is defined as the limit of the following expression:

$$\lim_{\omega\to\infty} T_*[H_\omega]. \tag{32}$$

It is pointed out in [22] that, when a convergent value is obtained by the self-cancellation method, the Abel-summed integral also converges, and they yield the same result.

By applying the self-cancellation method to H_{1tt} and taking into account the second and third terms on the right-hand side of (22), we obtain the numerical results of $G_{1\mathrm{tt,rem,k}}$. Figure 4 presents the numerical results of $G_{1\mathrm{tt,rem,k}}$ for $r = r_0$ with $m = m_0$. From Fig. 4, we observe that $G_{1\mathrm{tt,rem,k}}$ converges to a constant as k increases. This indicates that the self-cancellation method has successfully eliminated oscillations, yielding a convergent result. By comparing Figs. 1 and 4, we observe that the numerical magnitude changes from 10^3 to 10^{-5}, indicating that high precision must be maintained when solving the mode functions (17).

By repeating the above procedure, we can obtain the numerical results for all $G_{iuv,\mathrm{rem}}$ and G_{rem}. By taking them into (21), we obtain the expectation value of the renormalized stress-energy tensor $T_{uv,\mathrm{rem}}$ at the wormhole throat.

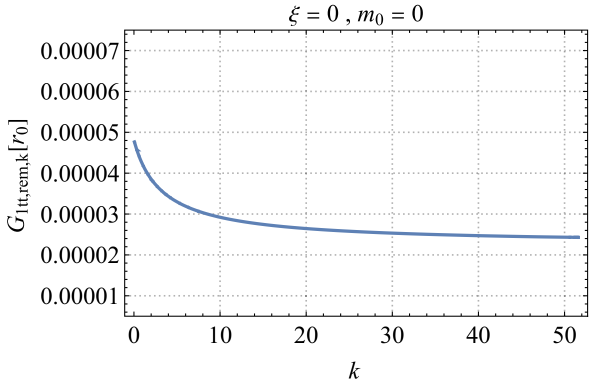

FIG. 4. The curve in this figure displays the value of $G_{1\mathrm{tt,rem,k}}$ for $r = r_0$, $\xi = 0$, and $m_0 = 0$ in the zero-tidal wormhole.

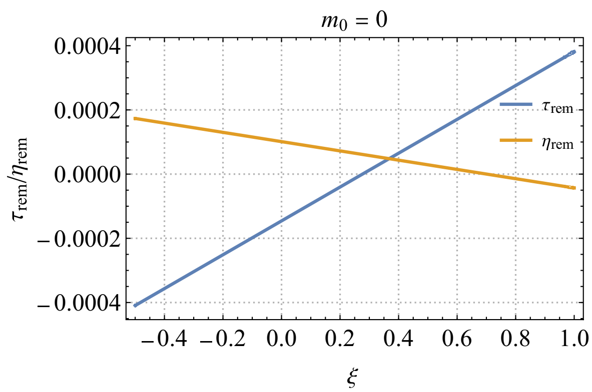

FIG. 5. The curves in this figure display the numerical values of τ_{rem} and η_{rem} for $m_0 = 0$.

Now, we can check whether the expectation value of the quantum vacuum stress-energy tensor can satisfy the Morris-Thorne conditions given by (6) and (7). We define

$$\tau_{\mathrm{rem}} = -T_{r_* r_*,\mathrm{rem}}(r_0), \tag{33}$$

$$\eta_{\mathrm{rem}} = -T_{\mathrm{tt,rem}}(r_0) - T_{r_* r_*,\mathrm{rem}}(r_0). \tag{34}$$

Figure 5 presents the numerical results of τ_{rem} and η_{rem} for $m_0 = 0$. From Fig. 5, we observe that there exists a parameter interval for ξ where $\tau_{\mathrm{rem}} > 0$ and $\eta_{\mathrm{rem}} > 0$. When the coupling constant ξ lies within this interval, the quantum vacuum stress-energy tensor tends to maintain the wormhole structure. When the coupling constant ξ lies outside this interval, the quantum vacuum stress-energy tensor tends to disrupt the wormhole structure. Thus, we find that, for the massless case, the coupling constant ξ plays opposite roles in wormhole stability across different parameter regions.

To systematically investigate the impact of dimensionless scalar field mass $m_0 b_0$ and coupling constant ξ on the stability of the wormhole throat, we perform calculations for various parameter values to explore whether the vacuum renormalized energy-momentum tensor satisfies

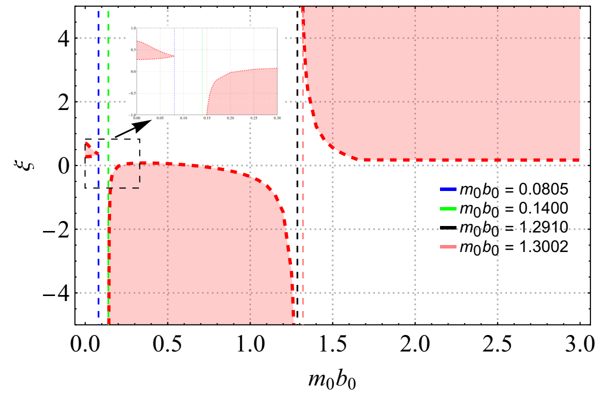

FIG. 6. This figure illustrates how the Morris-Thorne conditions depend on the dimensionless scalar field mass $m_0 b_0$ and the coupling constant ξ. The red regions indicate where the Morris-Thorne conditions are satisfied.

the Morris-Thorne conditions. In Fig. 6, we explore the Morris-Thorne conditions in the parameter space spanned by the dimensionless scalar field mass $m_0 b_0$ and coupling constant ξ. The red regions indicate that the renormalized energy-momentum tensor satisfies the Morris-Thorne conditions, thereby maintaining the wormhole structure. Figure 6 clearly reveals three disconnected regions satisfying the Morris-Thorne conditions. There exist four critical masses, $m_1 b_0 = 0.0805$, $m_2 b_0 = 0.1400$, $m_3 b_0 = 1.2910$, and $m_4 b_0 = 1.3002$. When $m_0 b_0 > m_4 b_0$, the Morris-Thorne conditions are satisfied only for $\xi > 0$, corresponding to the upper-right red region in Fig. 6. In this parameter regime, the associated vacuum stress-energy tensor tends to support the wormhole structure. When the dimensionless scalar field mass $m_0 b_0$ lies in the range $m_2 b_0 < m_0 b_0 < m_3 b_0$, the set of allowed ξ values is overwhelmingly dominated by negative coupling constants, with positive instances constituting a negligible minority. This corresponds to the red area in the bottom-left part of Fig. 6. If the scalar field parameters lie in this region, its vacuum stress-energy tensor tends to support the wormhole structure. When $0 < m_0 b_0 < m_1 b_0$, there is a small parameter window allowing the Morris-Thorne conditions to hold.

It is interesting to note that there exist two intervals $I_{\mathrm{ex1}} = (m_1 b_0, m_2 b_0)$ and $I_{\mathrm{ex2}} = (m_3 b_0, m_4 b_0)$ such that, when $m_0 b_0 \in I_{\mathrm{ex1}} \cup I_{\mathrm{ex2}}$, no value of the coupling constant ξ can satisfy the Morris-Thorne conditions. Thus, the union $I_{\mathrm{ex1}} \cup I_{\mathrm{ex2}}$ represents a strict no-go regime for wormhole solutions.

V. CONCLUSIONS

In this paper, we study the renormalized stress-energy tensor of a nonminimally coupled massive scalar field in a zero-tidal wormhole. Within the Hadamard renormalization framework, we numerically calculate the renormalized stress-energy tensor using the pragmatic mode-sum regularization method recently established by Levi and

Ori [22,23]. By varying the dimensionless scalar field mass $m_0 b_0$ and coupling constant ξ, we identify the parameter regions in the $m_0 b_0$-ξ space where the Morris-Thorne conditions hold. These results are presented in Fig. 6.

As shown in Fig. 6, the dimensionless scalar field mass $m_0 b_0$ and coupling constant ξ exert a nontrivial influence on the Morris-Thorne conditions. There exist three disconnected parameter regions that satisfy the Morris-Thorne conditions. For $m_0 b_0 > m_4 b_0$, the Morris-Thorne conditions are satisfied only for $\xi > 0$. However, for $m_2 b_0 < m_0 b_0 < m_3 b_0$, the vast majority of ξ values that satisfy the Morris-Thorne conditions are negative. Furthermore, within the interval $0 < m_0 b_0 < m_1 b_0$, there exists a parameter region that is significantly smaller than the other two regions and satisfies the Morris-Thorne conditions. When $m_0 b_0 \in (m_1 b_0, m_2 b_0) \cup (m_3 b_0, m_4 b_0)$, no value of ξ can satisfy the Morris-Thorne conditions. Thus, this set constitutes a no-go regime for traversable wormhole solutions.

Our results demonstrate that the renormalized energy-momentum tensor can satisfy the Morris-Thorne conditions across a broad range of parameters. Consequently, within these parameter regions, the renormalized energy-momentum tensor tends to maintain the wormhole structure. This suggests the possibility of utilizing the quantum vacuum of a scalar field to construct wormholes. On the other hand, we also identify two parameter regions that together constitute a no-go regime for traversable wormhole solutions. Through straightforward dimensional analysis [26,27], the natural scale of semiclassical vacuum wormholes must be at or even smaller than the Planck length. As pointed out in [14], in order to obtain semiclassical wormholes having scales larger than Planckian, one may need to consider thermal states at temperature T or vacuum polarizations (the Casimir effect) with additional boundary constraints on a typical scale R. In both cases, there exist extra macroscopic dimensional parameters. We intend to explore these scenarios in our future work.

ACKNOWLEDGMENTS

S. J. is supported by the National Natural Science Foundation of China with Grant No. 12275087 and J. J. is supported by the National Natural Science Foundation of China with Grant No. 12205014.

DATA AVAILABILITY

The data supporting this study's findings are available within the article.

APPENDIX A: HADAMARD RENORMALIZATION OF THE ENERGY-MOMENTUM TENSOR

In this appendix, we will discuss the singularity structure of the two-point correlation function, namely the Hadamard condition, as well as the expression of the renormalized energy-momentum tensor under the Hadamard renormalization scheme.

In Sec. III, we introduce the field operator $\hat{\phi}(x)$ and vacuum state $|0\rangle$. Then, we may calculate the vacuum expectation value of $\hat{\phi}^2$, and its expression is

$$\langle 0|\hat{\phi}^2(x)|0\rangle = \int_0^\infty dk \sum_{l=0}^{\infty} \sum_{m=-l}^{m=l} \Big(\psi^{L*}_{\omega(k)lm}(x)\psi^{L}_{\omega(k)lm}(x) + \psi^{R*}_{\omega(k)lm}(x)\psi^{R}_{\omega(k)lm}(x) \Big). \tag{A1}$$

However, one may find that this expression diverges. This is because physically reasonable states need to satisfy the Hadamard condition [29–31], which describes the short-distance singular behavior of the two-point correlation function. It is useful to introduce a few concepts before presenting the Hadamard condition. The convex normal neighborhood is a globally hyperbolic subspacetime $U \subset M$ such that any $x, x' \in U$ can be connected by a unique geodesic within U. For any $x, x' \in U$, we can define the signed squared geodesic distance $\sigma(x, x')$ uniquely [29]. Since U is a time oriented subspacetime, we can define a time function $T(x)$ on U. The Hadamard condition can be defined as follows [31]. For any $x, x' \in U$, the two-point correlation function $\omega_2(x, x')$ has the general form

$$\omega_2(x, x') = \lim_{\epsilon \to 0^+} \frac{1}{4\pi^2} \left(\frac{\Delta^{\frac{1}{2}}(x, x')}{\sigma + i\epsilon T} + V(x, x') \times \log(\sigma + i\epsilon T) + W_\omega(x, x') \right), \tag{A2}$$

where $\Delta^{1/2}$ is the square root of Van Vleck–Morette determinant, V can be obtained by Hadamard recursion relation [32], $T = T(x) - T(x')$, W_ω is a state-dependent smooth function on $U \times U$, and $\epsilon \to 0$ in the distribution sense.

It should be noted that the first two terms on the right-hand side of Eq. (A2) exhibit singular behavior when $x \to x'$. Because of this singular behavior, the expression (A1) diverges and requires renormalization. Fortunately, $\Delta^{1/2}$ and V are determined uniquely by the local geometry, which makes renormalization possible.

In this paper, we use the Hadamard renormalization scheme [24]. First, let us recall how to obtain the renormalized expectation values of $\hat{\phi}^2$ within the Hadamard framework. For convenience, we use the symmetric two-point function to eliminate the ϵ part in (A2). The symmetric two-point function is defined by

$$\omega_{2,\mathrm{sym}} = \frac{1}{2}(\omega_2(x, x') + (\omega_2(x', x)). \tag{A3}$$

For any two-point correlation function $\omega_2(x, x')$ given in (A2), the corresponding renormalized vacuum expectation value of $\hat{\phi}^2$ is formally given by

$$\omega_{2,\mathrm{rem}}(x) = \lim_{x'\to x}\omega_{2,\mathrm{sym}} - C(x,x') = \lim_{x'\to x}\frac{1}{4\pi^2}W_\omega(x,x'), \tag{A4}$$

where the symbol $\omega_{2,\mathrm{rem}}$ represents the corresponding renormalized vacuum expectation value of $\hat{\phi}^2$ and $C(x,x')$ is given by

$$C(x,x') = \frac{1}{4\pi^2}\left(\frac{\Delta^{\frac{1}{2}}(x,x')}{\sigma} + V(x,x')\log|\sigma|\right). \tag{A5}$$

Similarly, according to the expression of the classical energy-momentum tensor (11), the renormalized vacuum energy-momentum tensor $T_{uv,\mathrm{rem}}$ can be written as

$$\begin{aligned} T_{uv,\mathrm{rem}}(x) &= \lim_{x'\to x}\tilde{T}_{uv}(x,x')\left[\frac{1}{2}(\omega_2(x,x') + \omega_2(x',x)) - C(x,x')\right] + \frac{v_1}{4\pi^2}g_{uv} \\ &= \lim_{x'\to x}\frac{1}{4\pi^2}\tilde{T}_{uv}(x,x')W_\omega(x,x') + \frac{v_1}{4\pi^2}g_{uv}, \end{aligned} \tag{A6}$$

where the second term on the right-hand side corresponds to the trace anomaly [33] and the $\tilde{T}_{uv}(x,x')$ is given by [24]

$$\begin{aligned} \tilde{T}_{uv}(x,x') = {}& (1-2\xi)g_v{}^{v'}\nabla_u\nabla_{v'} + \left(2\xi - \frac{1}{2}\right)g_{uv}g^{\rho\sigma'}\nabla_\rho\nabla_{\sigma'} - 2\xi g_u{}^{u'}g_v{}^{v'}\nabla_{u'}\nabla_{v'} \\ & + 2\xi g_{uv}\nabla_\rho\nabla^\rho + \xi\left(R_{uv} - \frac{1}{2}Rg_{uv}\right) - \frac{1}{2}m_0^2 g_{uv}, \end{aligned} \tag{A7}$$

where $g_u{}^{u'}$ is the bivector of parallel displacement [19].

In practice, we know that expressions are represented in the form of mode functions, such as (A1), rather than in the form presented in (A2). Therefore, we cannot obtain the analytical expression for $W_\omega(x,x')$ and it is convenient to utilize the first line of (A6) for the calculation. For convenience, we define the symmetrized two-point correlation function, which can be written as

$$G(x,x') = \langle 0|\left[\hat{\phi}(x),\hat{\phi}(x')\right]_+|0\rangle = \int_0^\infty dk\sum_{l=0}^{\infty}\sum_{m=-l}^{m=l}\left(\{\psi^{L*}_{\omega(k)lm}(x),\psi^{L}_{\omega(k)lm}(x')\} + \{\psi^{R*}_{\omega(k)lm}(x),\psi^{R}_{\omega(k)lm}(x')\}\right), \tag{A8}$$

where

$$\left[\hat{\phi}(x),\hat{\phi}(x')\right]_+ = \frac{1}{2}\left(\hat{\phi}(x)\hat{\phi}(x') + \hat{\phi}(x')\hat{\phi}(x)\right) \tag{A9}$$

and

$$\{X(x),Y(x')\} = \frac{1}{2}(X(x)Y(x') + Y(x)X(x')). \tag{A10}$$

Similarly, the derivative $\nabla_u\nabla'_v$ of the symmetrized two-point correlation function is given by

$$\begin{aligned} G(x,x')_{;uv'} &= \langle 0|\left[\nabla_u\hat{\phi}(x),\nabla_{v'}\hat{\phi}(x')\right]_+|0\rangle \\ &= \int_0^\infty dk\sum_{l=0}^{\infty}\sum_{m=-l}^{m=l}\left(\{\psi^{L*}_{\omega(k)lm}(x),\psi^{L}_{\omega(k)lm}(x')\}_{;uv'} + \{\psi^{R*}_{\omega(k)lm}(x),\psi^{R}_{\omega(k)lm}(x')\}_{;uv'}\right). \end{aligned} \tag{A11}$$

Other derivatives can be obtained in a similar manner. Thus, the expression of $\tilde{T}_{uv,\mathrm{rem}}$ can be rewritten as

$$\begin{aligned}\tilde{T}_{uv,\mathrm{rem}}(x) = \lim_{x'\to x}\Bigg[&(1-2\xi)\left(g_v{}^{v'}G(x,x')_{;uv'} - g_v{}^{v'}C(x,x')_{;uv'}\right)\\ &+\left(2\xi-\frac{1}{2}\right)g_{uv}\left(g^{\rho\sigma'}G(x,x')_{;\rho\sigma'} - g^{\rho\sigma'}C(x,x')_{;\rho\sigma'}\right) - 2\xi\left(g_u{}^{u'}g_v{}^{v'}G(x,x')_{;u'v'} - g_u{}^{u'}g_v{}^{v'}C(x,x')_{;u'v'}\right)\\ &+2\xi g_{uv}(G(x,x')_{;\rho}{}^{;\rho} - C(x,x')_{;\rho}{}^{;\rho}) + \xi\left(R_{uv} - \frac{1}{2}Rg_{uv}\right)(G(x,x') - C(x,x')) - \frac{1}{2}m_0^2 g_{uv}(G(x,x') - C(x,x'))\Bigg].\end{aligned} \tag{A12}$$

Here $G(x,x')$ and its derivative can be obtained by solving the radial equation (13) numerically, while $C(x,x')$ and its derivative can be obtained using the method developed in [19,24].

APPENDIX B: EXPLICIT EXPRESSIONS FOR THE RENORMALIZED ENERGY-MOMENTUM TENSOR

In this appendix, we need to rewrite the formula (20) into a form more conducive to numerical computation. Here are four types of terms in (20), which can be written as

$$\begin{aligned}&1.\ \lim_{x'\to x}\left(g_v{}^{v'}G(x,x')_{;uv'} - g_v{}^{v'}C(x,x')_{;uv'}\right),\\ &2.\ \lim_{x'\to x}\left(g_u{}^{u'}g_v{}^{v'}G(x,x')_{;u'v'} - g_u{}^{u'}g_v{}^{v'}C(x,x')_{;u'v'}\right),\\ &3.\ \lim_{x'\to x}(G(x,x')_{;uv} - C(x,x')_{;uv}),\\ &4.\ \lim_{x'\to x}(G(x,x') - C(x,x')).\end{aligned} \tag{B1}$$

Let us consider the first term of (B1), which can be expressed as

$$G_{1uv,\mathrm{rem}}(x) = \lim_{x'\to x}\left(g_v{}^{v'}G(x,x')_{;uv'} - C_{1uv}(x,x')\right), \tag{B2}$$

where

$$C_{1uv}(x,x') = g_v{}^{v'}C(x,x')_{;uv'}. \tag{B3}$$

As pointed out in [23], for the sake of computational convenience, we rewrite (B2) as

$$G_{1uv,\mathrm{rem}}(x) = \lim_{x'\to x}\left(G_{1uv}(x,x') - (g^{-1})_v{}^{\sigma}C_{1u\sigma}(x,x')\right). \tag{B4}$$

Here, $G_{1uv}(x,x')$ means we use the coordinate system of point x to take the covariant derivative with respect to both x and x' once each.

Similarly, the second term of (B1) can be written as

$$G_{2uv,\mathrm{rem}}(x) = \lim_{x'\to x}\left(G_{2uv}(x,x') - (g^{-1})_u{}^{\rho}(g^{-1})_v{}^{\tau}C_{2\rho\tau}(x,x')\right) \tag{B5}$$

and the third term term of (B1) can be written as

$$G_{0uv,\mathrm{rem}}(x) = \lim_{x'\to x}(G_{0uv}(x,x') - C_{0uv}(x,x')), \tag{B6}$$

where

$$C_{2uv}(x,x') = g_u{}^{u'}g_v{}^{v'}C(x,x')_{;u'v'} \tag{B7}$$

and

$$C_{0uv}(x,x') = C(x,x')_{;uv}. \tag{B8}$$

Here, $G_{0uv}(x,x')$ corresponds to taking the covariant derivative twice with respect to x using the coordinate system of point x. Similarly, $G_{2uv}(x,x')$ corresponds to taking the covariant derivative twice with respect to x' using the coordinate system of point x.

Now, returning to (B2), since the spacetime is static, we separate the points in the t direction. We choose

$$x = (t,r,\theta,\varphi), \qquad x' = (t+\epsilon,r,\theta,\varphi). \tag{B9}$$

Then, the limit $x'\to x$ corresponds to $\epsilon\to 0$. Using (17), we have

$$\psi^{L/R}_{\omega lm}(x') = \psi^{L/R}_{\omega lm}(x)e^{-i\omega\epsilon}. \tag{B10}$$

Then, inserting (A11) into (B4), we get

$$G_{1uv,\mathrm{rem}}(x) = \lim_{\epsilon\to 0}\int_0^\infty F_{1uv}(x,k)\cos(\omega(k)\epsilon)dk - L_{1uv}(x,\epsilon), \tag{B11}$$

where

$$F_{1uv}(x,k) = \sum_{l=0}^{\infty}\sum_{m=-l}^{m=l}\Big(\{\psi^{L*}_{\omega(k)lm,u}(x), \psi^{L}_{\omega(k)lm,v}(x)\} + \{\psi^{R*}_{\omega(k)lm,u}(x), \psi^{R}_{\omega(k)lm,v}(x)\}\Big) \tag{B12}$$

and

$$L_{1uv}(x,\epsilon) = (g^{-1})_v{}^{\sigma} C_{1u\sigma}(x,x'). \tag{B13}$$

The specific expression of $L_{1uv}(x,\epsilon)$ can be obtained through the method in [19], and its general form can be written as

$$L_{1uv}(x,\epsilon) = \frac{a_{1uv}(x)}{\epsilon^4} + \frac{b_{1uv}(x)}{\epsilon^2} + \frac{c_{1uv}(x)}{\epsilon} + d_{1uv}(x)\log(|\sigma|) + e_{1uv}(x) + O(\epsilon). \tag{B14}$$

It is convenient to rewrite the expression for $L_{1uv}(x,\epsilon)$ in integral form. To achieve it, we can utilize the following identities [11,23]:

$$\begin{aligned}
\int_0^\infty \omega^3\cos(\omega\epsilon)d\omega &= \frac{6}{\epsilon^4},\\
\int_0^\infty \omega\cos(\omega\epsilon)d\omega &= -\frac{1}{\epsilon^2},\\
\int_0^\infty \log(\sigma)\cos(\omega\epsilon)d\omega &= -\frac{\pi}{2\epsilon},\\
\int_0^\infty \frac{1}{\omega+\mu e^{-\gamma}}\cos(\omega\epsilon)d\omega &= -\log(\mu\epsilon) + O(\epsilon),
\end{aligned} \tag{B15}$$

where γ is the Euler constant. Then, we can rewrite (B11) as

$$\begin{aligned}
G_{1uv,\mathrm{rem}}(x) &= \lim_{\epsilon\to 0}\int_0^\infty F_{1uv}(x,k)\cos(\omega(k)\epsilon)dk - \lim_{\epsilon\to 0}\int_0^\infty F_{1uv,\mathrm{sing}}(x,\omega(k))\cos(\omega(k)\epsilon)d\omega - e_{1uv}(x)\\
&= \lim_{\epsilon\to 0}\int_0^\infty \left[F_{1uv}(x,k) - \frac{k}{\sqrt{k^2+m_0^2}}F_{1uv,\mathrm{sing}}(x,\omega(k))\right]\cos(\omega(k)\epsilon)dk\\
&\quad - \lim_{\epsilon\to 0}\int_0^m F_{1uv,\mathrm{sing}}(x,\omega(k))\cos(\omega(k)\epsilon)d\omega - e_{1uv}(x),
\end{aligned} \tag{B16}$$

where

$$F_{1uv,\mathrm{sing}}(x,\omega) = \frac{1}{6}a_{1uv}(x)\omega^3 - b_{1uv}(x)\omega - \frac{2}{\pi}c_{1uv}(x)\log(\omega) - d_{1uv}(x)\frac{1}{\omega+e^{-\gamma}}. \tag{B17}$$

The limit and integral order can be directly exchanged in the third line of (B16), whereas the interchange in the second line of (B16) is nontrivial. We need to employ the self-cancellation technique developed in [22,23] to handle this integral. By treating this integral as a generalized integral and applying self-cancellation to it, we can take the limit. Thus, we have

$$G_{1uv,\mathrm{rem}}(x) = \int_0^\infty \left[F_{1uv}(x,k) - \frac{k}{\sqrt{k^2+m_0^2}}F_{1uv,\mathrm{sing}}(x,\omega(k))\right]dk - \int_0^{m_0} F_{1uv,\mathrm{sing}}(x,\omega(k))d\omega - e_{1uv}(x). \tag{B18}$$

This gives the final computational form for the first term of (B1). Similarly, the expressions for the second and third terms of (B1) can be written as

$$G_{2uv,\mathrm{rem}}(x) = \int_0^\infty \left[F_{2uv}(x,k) - \frac{k}{\sqrt{k^2+m_0^2}}F_{2uv,\mathrm{sing}}(x,\omega(k))\right]dk - \int_0^{m_0} F_{2uv,\mathrm{sing}}(x,\omega(k))d\omega - e_{2uv}(x) \tag{B19}$$

and

$$G_{0uv,\mathrm{rem}}(x) = \int_0^\infty \left[F_{0uv}(x,k) - \frac{k}{\sqrt{k^2+m_0^2}}F_{0uv,\mathrm{sing}}(x,\omega(k))\right]dk - \int_0^{m_0} F_{0uv,\mathrm{sing}}(x,\omega(k))d\omega - e_{0uv}(x), \tag{B20}$$

where

$$F_{2uv}(x,k) = \sum_{l=0}^{\infty}\sum_{m=-l}^{m=l}\Big(\{\psi^{L*}_{\omega(k)lm}(x), \psi^{L}_{\omega(k)lm;uv}(x)\} + \{\psi^{R*}_{\omega(k)lm}(x), \psi^{R}_{\omega(k)lm;uv}(x)\}\Big) \tag{B21}$$

and

$$F_{0uv}(x,k) = \sum_{l=0}^{\infty}\sum_{m=-l}^{m=l}\left(\{\psi^{L*}_{\omega(k)lm;uv}(x),\psi^{L}_{\omega(k)lm}(x)\} + \{\psi^{R*}_{\omega(k)lm;uv}(x),\psi^{R}_{\omega(k)lm}(x)\}\right). \tag{B22}$$

Now we consider the fourth term of (B1), which can be written as

$$\begin{aligned} G_{\mathrm{rem}}(x) &= \lim_{x'\to x}(G(x,x') - C(x,x')) \\ &= \int_0^\infty \left[F(x,k) - \frac{k}{\sqrt{k^2+m_0^2}}F_{\mathrm{sing}}(x,\omega(k))\right]dk - \int_0^m F_{\mathrm{sing}}(x,\omega(k))d\omega - e(x), \end{aligned} \tag{B23}$$

where

$$F(x,k) = \sum_{l=0}^{\infty}\sum_{m=-l}^{m=l}\left(|\psi^{L}_{\omega(k)lm}(x)|^2 + |\psi^{R}_{\omega(k)lm}(x)|^2\right) \tag{B24}$$

and

$$F_{\mathrm{sing}}(x,\omega) = -b(x)\omega - \frac{2}{\pi}c(x)\log(\omega) - d(x)\frac{1}{\omega + e^{-\gamma}}. \tag{B25}$$

The $F_{iuv,\mathrm{sing}}$ and F can be derived via the method outlined in [19], combined with the explicit geometric forms given in [24]. After some calculations, we obtain

$$\begin{aligned}
&a_{0tt} = a_{2tt} = -a_{1tt} = -\frac{3}{2\pi^2}, \qquad b_{0tt} = b_{2tt} = -b_{1tt} = -\frac{m_0^2}{8\pi^2}, \qquad c_{0tt} = c_{2tt} = -c_{1tt} = 0, \\
&d_{0tt} = d_{2tt} = -d_{1tt} = -\frac{1+20m_0^4r^6}{640\pi^2r^6}, \qquad e_{0tt} = e_{2tt} = -e_{1tt} = \frac{(1+20m_0^4r^6)(-3+\log 2)}{1280\pi^2r^6}, \\
&a_{0r_*r_*} = a_{2r_*r_*} = -a_{1r_*r_*} = -\frac{1}{2\pi^2}, \qquad b_{0r_*r_*} = b_{2r_*r_*} = -b_{1r_*r_*} = \frac{1-3m_0^2r^3}{24\pi^2r^3}, \\
&c_{0r_*r_*} = c_{2r_*r_*} = -c_{1r_*r_*} = 0, \qquad d_{0r_*r_*} = d_{2r_*r_*} = -d_{1r_*r_*} = \frac{1-40m_0^2r^3+60m_0^4r^6}{1920\pi^2r^6}, \\
&e_{0r_*r_*} = e_{2r_*r_*} = -e_{1r_*r_*} = -\frac{-3+60m_0^4r^6(-1+\log 2)+\log 2-40m_0^2r^3\log 2}{3840\pi^2r^6}, \\
&a_{0\varphi\varphi} = a_{2\varphi\varphi} = -a_{1\varphi\varphi} = -\frac{r^2}{2\pi^2}, \qquad b_{0\varphi\varphi} = b_{2\varphi\varphi} = -b_{1\varphi\varphi} = -\frac{1+6m_0^2r^3}{48\pi^2r}, \\
&c_{0\varphi\varphi} = c_{2\varphi\varphi} = -c_{1\varphi\varphi} = 0, \qquad d_{0\varphi\varphi} = d_{2\varphi\varphi} = -d_{1\varphi\varphi} = \frac{-1+10m_0^2r^3+30m_0^4r^6}{960\pi^2r^4}, \\
&e_{0\varphi\varphi} = e_{2\varphi\varphi} = -e_{1\varphi\varphi} = \frac{3-60m_0^4r^6(-1+\log 2)-20m_0^2r^3\log 2+\log 4}{3840\pi^2r^4}, \\
&b = -\frac{1}{4\pi^2}, \qquad c = 0, \qquad d = \frac{m_0^2}{8\pi^2}, \qquad e = -\frac{m_0^2\log 2}{16\pi^2}.
\end{aligned} \tag{B26}$$

[1] M. S. Morris and K. S. Thorne, Am. J. Phys. **56**, 395 (1988).
[2] M. S. Morris, K. S. Thorne, and U. Yurtsever, Phys. Rev. Lett. **61**, 1446 (1988).
[3] B. E. Taylor, W. A. Hiscock, and P. R. Anderson, Phys. Rev. D **55**, 6116 (1997).
[4] J. Matyjasek, Phys. Rev. D **102**, 024082 (2020).
[5] A. A. Popov, Classical Quantum Gravity **22**, 5223 (2005).
[6] E. D. Carlson, P. R. Anderson, A. Fabbri, S. Fagnocchi, W. H. Hirsch, and S. Klyap, Phys. Rev. D **82**, 124070 (2010).
[7] E. Kocuper, J. Matyjasek, and K. Zwierzchowska, Phys. Rev. D **96**, 104057 (2017).
[8] A. A. Popov, Phys. Rev. D **64**, 104005 (2001).
[9] N. R. Khusnutdinov, Phys. Rev. D **67**, 124020 (2003).
[10] A. A. Popov and S. V. Sushkov, Phys. Rev. D **63**, 044017 (2001).
[11] P. R. Anderson, W. A. Hiscock, and D. A. Samuel, Phys. Rev. D **51**, 4337 (1995).
[12] D. Hochberg, A. Popov, and S. V. Sushkov, Phys. Rev. Lett. **78**, 2050 (1997).
[13] D. Lisenkov and A. Popov, Symmetry **15**, 426 (2023).
[14] A. R. Khabibullin, N. R. Khusnutdinov, and S. V. Sushkov, Classical Quantum Gravity **23**, 627 (2006).
[15] L. M. Butcher, Phys. Rev. D **90**, 024019 (2014).
[16] V. B. Bezerra, E. R. Bezerra de Mello, N. R. Khusnutdinov, and S. V. Sushkov, Phys. Rev. D **81**, 084034 (2010).
[17] J. S. Schwinger, Phys. Rev. **82**, 664 (1951).
[18] B. S. DeWitt, Conf. Proc. C **630701**, 585 (1964).
[19] S. M. Christensen, Phys. Rev. D **14**, 2490 (1976).
[20] P. Candelas and K. W. Howard, Phys. Rev. D **29**, 1618 (1984).
[21] K. W. Howard, Phys. Rev. D **30**, 2532 (1984).
[22] A. Levi and A. Ori, Phys. Rev. D **91**, 104028 (2015).
[23] A. Levi, Phys. Rev. D **95**, 025007 (2017).
[24] Y. Decanini and A. Folacci, Phys. Rev. D **78**, 044025 (2008).
[25] B. S. DeWitt, Phys. Rep. **19**, 295 (1975).
[26] L. H. Ford and T. A. Roman, Phys. Rev. D **53**, 5496 (1996).
[27] K. K. Nandi, Y. Z. Zhang, and K. B. Vijaya Kumar, Phys. Rev. D **70**, 064018 (2004).
[28] [DATA REFERENCE].
[29] M. J. Radzikowski, Commun. Math. Phys. **179**, 529 (1996).
[30] S. Hollands, R. M. Wald, and J. Zahn, Classical Quantum Gravity **37**, 115009 (2020).
[31] B. S. Kay and R. M. Wald, Phys. Rep. **207**, 49 (1991).
[32] B. S. DeWitt and R. W. Brehme, Ann. Phys. (N.Y.) **9**, 220 (1960).
[33] R. M. Wald, Phys. Rev. D **17**, 1477 (1978).